30th International Conference
ENGINEERING MECHANICS 2024
Milovy, Czech Republic, May 14 – 16, 2024

OPTIMIZING VENTURI NOZZLE DESIGN FOR ENHANCED CAVITATION AND PRESSURE DYNAMICS: A COMPARATIVE ANALYSIS OF TURBULENCE MODELS FOR CAVITATING FLOW CHARACTERIZATION

Zeman R.*, Rudolf P.**

Abstract: *This article compares three Venturi nozzle geometries using CFD to determine the best geometry variant for enhanced cavitation and pressure pulsations. Simulations were performed using two different turbulence models, a hybrid SBES and a RANS model SST k-ω. Comparisons were made from the time recording of the vapor volume and pressure monitors. Changing the turbulence model led to different results, and therefore the outputs of the more complex SBES model were considered as valid. Venturi nozzle with zero throat length was found to be the best choice at the selected boundary conditions for vapor phase formation while increasing amplitudes of pressure pulsations.*

Keywords: Cavitation, CFD, Venturi, pulsations.

1. Introduction

Cavitation has long been known for its negative effects especially during the operation of hydraulic machines. Vibrations, noise or cavitation erosion accompanying the formation and violent collapse of cavitation bubbles have therefore become a subject of numerous studies. Efforts have been made to fully or at least partially mitigate these negative effects. One of the ways for cavitation suppression is shape optimization of those machine parts which are susceptible to cavitation and cavitation erosion. (Epps, 2015 and Sun, 2022).

Recently, cavitation has been studied so that its destructive effects can in turn be used for the benefit of the cause. If cavitation is to be generated on purpose, it is desirable that the most intense cavitation possible occurs in the device, using as little energy as possible. This fact opens the door to shape optimization, which in turn will enhance cavitation and thus allow cavitation generators to become more efficient. Water purification using hydrodynamic cavitation is one of the areas of research (Dular, 2016), where venturi nozzles of different shapes are widely used for this purpose (Jančula, 2014). Improving the efficiency of these simple devices would promote their eventual deployment in industry.

2. Methods

All three nozzle geometries were designed with a circular cross-section, 0.5 mm wide throat, 5 mm wide upstream section, 3 mm wide downstream section and confuser section with 60 ° angle. Geometry variant A, Fig. 1, had a 2 mm long neck and a diffuser angle of 12 °, while variant B had a wider diffuser angle of 14 °. Variant C, while maintaining a diffuser angle of 12 °, lacked the full length of the throat and the converging part was therefore directly connected to the diffuser.

* Ing. Radek Zeman: Faculty of Mechanical Engineering, Brno University of Technology, Technická 2896/2; 616 69, Brno; CZ, 192038@vutbr.cz

** Assoc. Prof. Ing. Pavel Rudolf, PhD.: Faculty of Mechanical Engineering, Brno University of Technology, Technická 2896/2; 616 69, Brno; CZ, rudolf@fme.vutbr.cz

doi: 10.21495/em2024-326

Fluid domains were created for all three 3D geometries with appropriate decomposition. Structured conformal hexagonal meshes were then generated with respect to y+ not exceeding value of 5 in the regions of interest (nozzle throat and diffuser) during the simulation. The final meshes consisted of A) 4 050 000, B) 4 050 000 and C) 3 690 000 elements.

Y+ values for mesh sizing and boundary conditions were determined from preliminary simulation. The boundary conditions were chosen to enable testing of the manufactured nozzles in an available hydraulic laboratory if necessary. Prior to running the simulation, pressure monitors were set at 21 points located in the nozzle diffuser. The pressure at the inlet and the volume of the vapor phase in the fluid domain were also monitored. Simulations were performed with all three geometries in Ansys Fluent software using the hybrid turbulence model SBES and the two-equation RANS turbulence model SST k-ω. The boundary conditions correspond to the values of the Reynolds number $Re = 19\,904$ (1) and the cavitation number $\sigma = 0.124$ (2).

$$Re = \frac{D_H \cdot v_T}{\nu}\ [-], \tag{1}$$

$$\sigma = \frac{p_2 - p_V}{\rho \cdot \frac{v_T^2}{2}}\ [-], \tag{2}$$

where $D_H\ [m]$ denotes the hydraulic diameter of nozzle throat, $v_T\ [m \cdot s^{-1}]$ the mean velocity in nozzle throat, $\nu\ [m^2 \cdot s^{-1}]$ the kinematic viscosity of water, $p_2\ [Pa]$ the absolute pressure at the outlet, $p_V\ [Pa]$ the saturated water vapor pressure, $\rho\ [kg \cdot m^{-3}]$ the density of water.

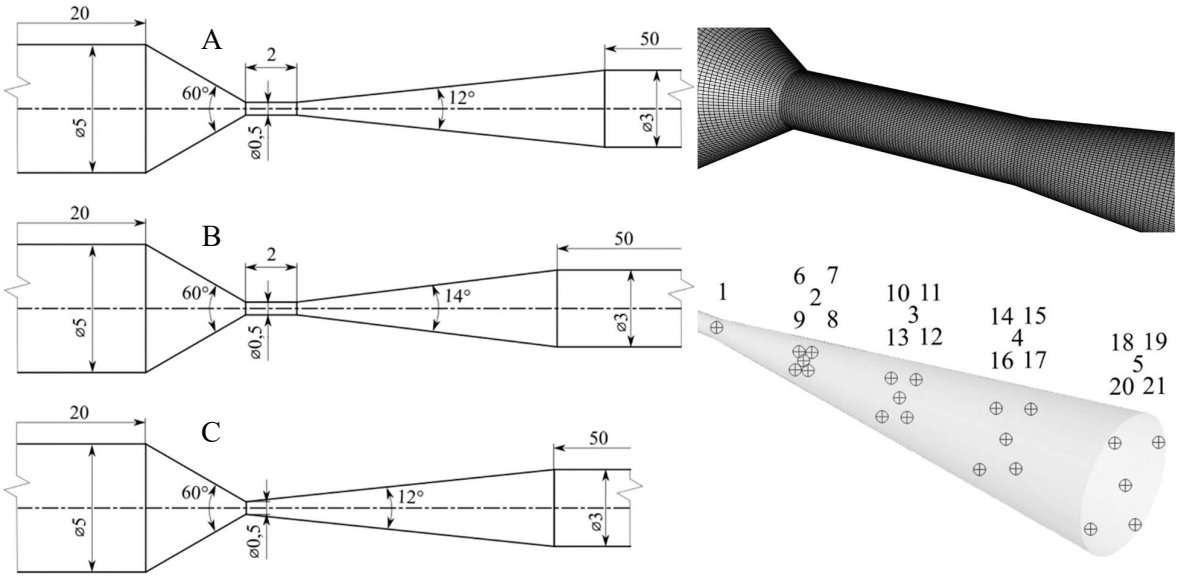

Fig. 1: Fluid domain geometry variants (on letf), mesh (upper right), pressure monitors (bottom right).

Although SBES has been called a hybrid turbulence model previously, it is more of a new way to combine existing RANS and LES models through the so-called shielding (blending) function (3):

$$\mu_T = \mu_T^{RANS} f_S + \mu_T^{LES}(1 - f_S) \tag{3}$$

The combination of RANS and LES is designed to model certain flow cases where conventional RANS would not produce accurate results (strong mixing, separation, etc.), while reducing the computational demands in comparison with LES simulations (Menter, 2018).

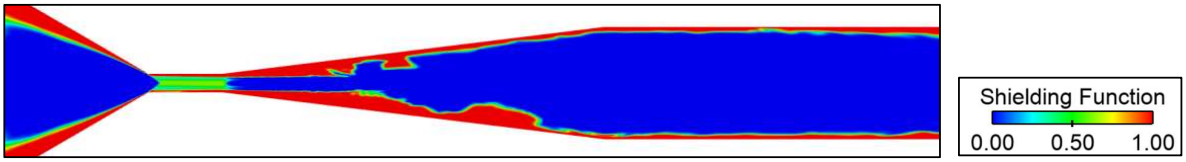

Fig. 2: Contour of shielding function for var B at maximum cavity length.

3. Results

The graphical representation of the vapour volume monitor (Figs. 3 and 4) showed a sinusoidal pattern for all three geometries, and for both the SBES and SST k-ω turbulence models. However the amplitudes of the sinusoids for the two selected turbulence models differed significantly for each nozzle design, sometimes by an order of magnitude (nozzle A and B). SBES predicted the highest amplitudes of the vapour phase change for geometry variant C, and smaller amplitudes for A and B, while the descending order of A, B ,C was determined by using the SST k-ω turbulence model.

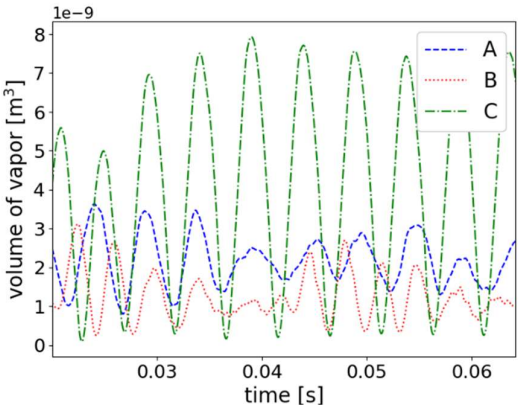

Fig. 3: SBES volume fraction monitor.

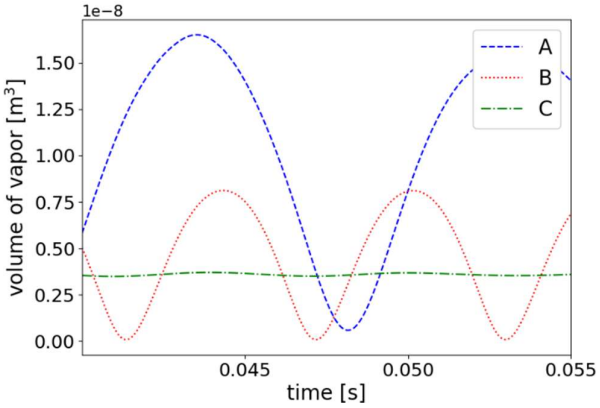

Fig. 4: SST k-ω volume fraction monitor.

The periodic change in the volume of the vapour phase corresponded with the typical behaviour of developed cavitation, where periodic shrinkage and growth of the cavity from the nozzle throat to the diffuser is usually observed. Except for variant A for SBES and variant C for SST k-ω, almost complete shrinkage of the cavity up to the nozzle neck always occurred during the simulation.

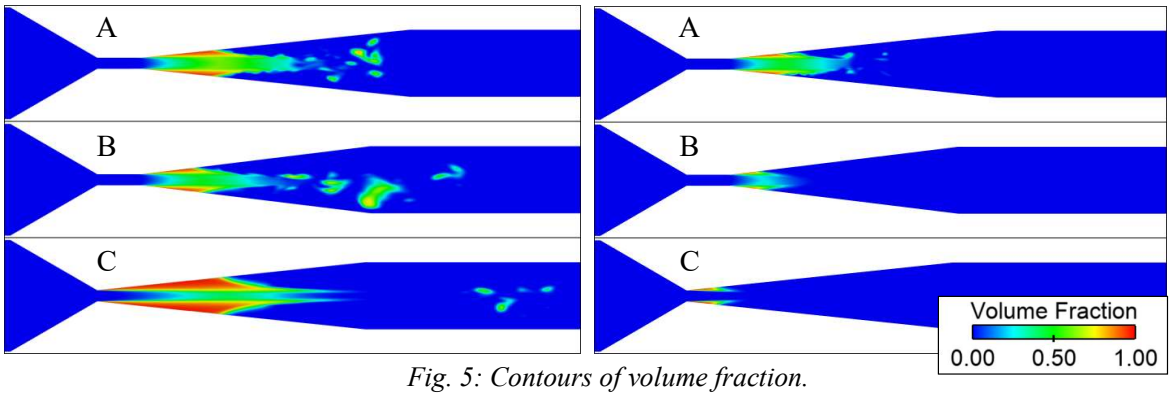

Fig. 5: Contours of volume fraction.

Fig. 5 shows the contours of the volume fraction for SBES simulation in a longitudinal section of each nozzle at the moment of cavity shrinkage and full expansion. The presence of separated parts of the vapor phase could also be observed on the contours. Pressure monitors showed that cavity shrinkage was accompanied by pressure pulsations as shown in Figs. 6 and 7. The amplitude of the pressure pulsations increased with increasing distance from the nozzle throat, while the amplitudes of a group of pressure monitors at the same distance from the throat (e.g. 2, 6, 7, 8, 9) did not differ significantly. SBES predicts a more credible pressure record compared to the smoother pattern coming from the RANS simulation. Secondary pulsations were probably caused by the collapse of the separated vapor fractions, which were present in the flow field only when using the hybrid turbulence model. The peaks of pressure pulsations were highest for SBES variant C, less so for B and A, while SST k-ω predicted a decreasing order of B, A and C.

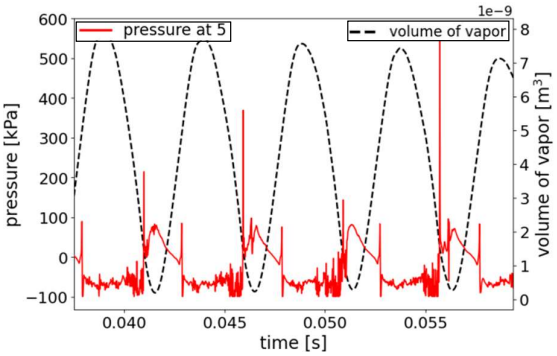

Fig. 6: SBES-monitor 5, C var.

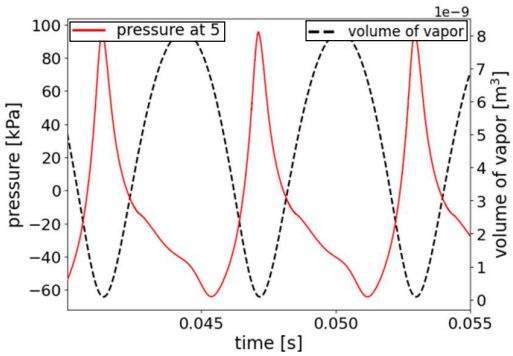

Fig. 7: SST k-ω-monitor 5, B var.

4. Conclusion

The CFD simulations showed different results when using different turbulence models. This could lead to the conclusion that the choice of turbulence model has a great influence on the results obtained from the simulations if cavitation is focus of interest. To confirm this, further CFD simulations would be needed to rule out the influence of the mesh on the results obtained, and even so, it would be necessary to perform experiments for final confirmation.

With the increase in computational complexity, SBES simulations should lead to more physical results, and therefore these results were considered as more reliable. SBES simulations showed that nozzle design C, i.e. without a throat, should be the best choice, whether the goal was to hold the highest possible volume of vapor phase in the nozzle or to create the highest pressure pulsations under the chosen boundary conditions.

Acknowledgement

Czech Science Foundation is acknowledged for support of the research under project 22-11456S „Exploring fundamental interactions of hydrodynamic cavitation and low-temperature plasma to enhance the disinfection effects“, conference attendance was supported by specific research project FSI-S-23-8183.

References

Dular, M. et al. (2016) Use of hydrodynamic cavitation in (waste)water treatment. *Ultrasonics Sonochemistry*, 29, pp. 577–588.

Epps, B., Víquez, O. and Chryssostomidis, C. (2015) A Method for Propeller Blade Optimization and Cavitation Inception Mitigation. *Journal of ship production and design*. 31, 2, pp. 88–98.

Jančula, D., Mikula, P., Maršálek, B., Rudolf, P. and Pochylý, F. (2014) Selective method for cyanobacterial bloom removal: hydraulic jet cavitation experience. *Aquaculture International*, 2 (22), pp. 509–521.

Menter, F. (2018) Stress-Blended Eddy Simulation (SBES) – A New Paradigm in Hybrid RANS-LES Modeling. In: *HRLM 2016: Progress in Hybrid RANS-LES Modelling*, pp. 27–37.

Sun, Z., Li, D., Mao, Y., Feng, L., Zhang, Y. and Liu, C. (2022) Anti-cavitation optimal design and experimental research on tidal turbines based on improved inverse BEM. *Energy* (Oxford), 239.